

Icy Soil Acquisition Device for the 2007 Phoenix Mars Lander

Philip Chu^{*}, Jack Wilson^{*}, Kiel Davis^{*}, Lori Shiraishi^{**} and Kevin Burke^{**}

Abstract

The Icy Soil Acquisition Device is a first of its kind mechanism that is designed to acquire ice-bearing soil from the surface of the Martian polar region and transfer the samples to analytical instruments, playing a critical role in the potential discovery of existing water on Mars. The device incorporates a number of novel features that further the state of the art in spacecraft design for harsh environments, sample acquisition and handling, and high-speed low torque mechanism design.

Introduction

The Phoenix Mars Mission, currently en route to Mars, consists of a lander equipped with tools and analytical instruments designed to assess the history of water and the habitability potential of the Martian polar ice-bearing soil. Icy soil is believed to exist in these regions underneath a shallow layer of regolith. The Phoenix lander includes a scoop mounted on the end of a robotic arm that will be used to remove the layer of loose soil covering ice-bearing materials. Once these materials are encountered, an ice-sampling tool within the scoop will penetrate and acquire icy soil samples that will then be delivered to analytical instruments by the Robotic Arm to ascertain the existence of water ice. The scoop and ice sampling tool is known as the Icy Soil Acquisition Device (ISAD). The ISAD is a first of its kind mechanism that will support the Thermal Evolved Gas Analyzer (TEGA) and the Microscopy, Electrochemistry and Conductivity Analyzer (MECA) experiments with critical soil samples.

The ISAD has two main functions; bulk digging of loose soil and precision sampling of hard ice-bearing soils. It is partitioned into two main chambers. The front chamber is used as a scoop, and performs the function of removing bulk material. The rear chamber contains a high-speed cutting tool, which penetrates and acquires harder icy soil. The two main chambers are separated by a series of panels. These panels prevent bulk material from filling the rear chamber of the ISAD during digging of loose soil, and also allow acquired icy soil to be transferred to the front chamber using a series of Robotic Arm wrist movements. A funnel feature in the front chamber allows for precision delivery of loose and icy soil to analytical instrument inlet ports. The ISAD also has two blades, the first attached to the front of the scoop, and the second attached to the bottom of the scoop, which are utilized for scraping surface regolith and ice.

When acquiring icy soil, the ISAD is preloaded against the surface so that the cutting bit is retracted into the scoop. The drivetrain is energized, rotating the cutting bit at high speed. Spring preload on the cutting bit forces it into the soil. Icy soil is ballistically ejected from the surface, into the rear chamber of the ISAD, where it is captured. Several samples can be acquired, after which the icy soil is transferred to the front chamber of the scoop using a series of Robotic Arm wrist motions. The sample is then delivered to science instruments by the Robotic Arm.

The ISAD is a first generation mechanism to be qualified for space flight. There are many aspects of the design that are unique, and should be brought to the attention of the spacecraft mechanism community. Many of these features will likely be used on subsequent missions, and this paper will provide details on their design, and lessons learned. This paper will first discuss the highly constrained design space dictated by the fact that the mechanism was a very late addition to the payload of the Phoenix Mars Lander. It will then give an overview of the ISAD device and its operational usage. The paper will discuss details of the design that are critical for understanding the lessons learned, and the unique features of the mechanism. Solutions to the constrained design space and lessons learned during design, assembly and testing will be presented in detail.

* Honeybee Robotics Spacecraft Mechanisms Corporation, New York, NY

** Jet Propulsion Laboratory, Pasadena, CA

Design Discussion

Driving Requirements

Prior to the ISAD, the planned method of acquiring ice-bearing soil samples used a set of passive blades mounted to the exterior of the Robotic Arm digging scoop. Once a layer of potentially icy soil was encountered, these blades would be dragged across the surface of the hard icy soil by the Robotic Arm to produce piles of loose material, which would then be acquired by the scoop and deposited at the instrument inlet ports. Several blade geometries were tested in dry analog material to determine the feasibility of the sample acquisition method. It was found that the method of scraping material and using the scoop to acquire it produced an insufficient amount of sample for the TEGA instrument within a reasonable amount of time. Due to potential sublimation loss of water ice, a faster, more productive method of sample acquisition was required. Honeybee Robotics Spacecraft Mechanisms Corporation was contracted by the Jet Propulsion Laboratory to provide an end-of-arm sample acquisition device that would produce at least an order of magnitude improvement on the passive scraping method, which had been generating on the order of tenths of cubic centimeters.

The ISAD was a late addition to the payload of the Phoenix Mars Lander. Most lander subsystems had already undergone their critical design reviews and were well into the fabrication, assembly and test phases by the time the ISAD was conceived. As a result, the ISAD had to comply with existing subsystems that had not been designed with an active end-of-arm sampling device in mind. This led to a number of requirements that tightly constrained the design space of the ISAD. These requirements, as well as a limited budget and rapid development schedule led to innovative design solutions and compromises.

One of the main drivers throughout the design process was the overall ISAD mass. The Robotic Arm was designed and analyzed to support a hollow scoop, with relatively light weight digging and scraping blades. The Robotic Arm's severe launch load environment required that the ISAD mass be limited to 0.75 kg in order to maintain sufficient strength margin.

The design of the ISAD was also limited by available resources of the lander electrical subsystem. There was one switched circuit available for an active device, limiting the device to one motor. A preset drive voltage of 24.6 to 29.3 VDC limited the speed of the motor to a narrow range of velocities. This voltage input was also unipolar, meaning that the ISAD would need to function unidirectionally. A restriction in the overall power available to the device resulted in a current limit of 1.0 Amp, causing a constraint on the available motor torque. Further constraining the amount of torque available for sampling was a requirement to start motion of the mechanism when preloaded against the ground with a torque margin of 1.0. Although an encoder was integral to the motor selected, there was no means of reading the encoder signal, resulting in an open loop device architecture, with no direct data feedback to tell if the device functioned properly. By reading the overall Robotic Arm subsystem power data, it could be determined that the device ran, however there would not be enough resolution in the data to calculate motor torque or speed. Due to limited budget and schedule resources, motor selection was limited to existing Jet Propulsion Laboratory flight spare stock from the Mars Exploration Rover project.

Productivity of the sampling device was also a key driver in the design process. The TEGA instrument requires at least 1 cm³ of icy soil material at its inlet ports to capture enough sample to perform an analysis. To fulfill this requirement, multiple sampling placements of the ISAD can be performed, however sublimation loss of water ice places a constraint on the total duration of these groups of sampling occurrences.

During the conceptual stage, it was determined that vibration greatly improved the movement of icy soil over metallic surfaces at Mars ambient temperature and pressure. This resulted in a self-imposed requirement for the device to produce its own vibration to help fluidize particles and move them over internal transfer surfaces.

Several other requirements placed constraints on the geometry, function and material choices of the device, including operational and survival temperatures (-80 °C to +45 °C and -108 °C to +110 °C respectively), required interior volume for digging operations (300 cm³), structural survival of digging loads during soil overburden removal, and surface coatings for thermal balance, durability and imaging.

Overview of Design

The ISAD is partitioned into two sections, a front and a rear chamber. The front chamber is used to collect bulk material acquired by scraping or digging, and transfer the soil overburden away from the main trench. Up to 310 cm³ of loose material may be collected in the front chamber at a time. A Primary Blade is attached to the front of the scoop that helps break up weak soil. The front chamber can also be used for precision drop-off of bulk soil to science instruments located on the lander deck. A funnel feature shown in Figure 2 channels acquired material into an 18.2-mm wide slot, improving the accuracy of sample delivery. The funnel and scoop geometry were designed to maintain functionality at lander tilts of up to 16° with respect to the local surface normal. The ISAD scoop and funnel feature are separate components and are made of 7075-T73 aluminum with a hard coat clear anodize for abrasion and wear resistance. This coating on the interior surfaces also reduces glare when viewing acquired samples with the Robotic Arm Camera. A tungsten carbide secondary blade on the bottom side of the scoop provides a means of penetrating harder materials.

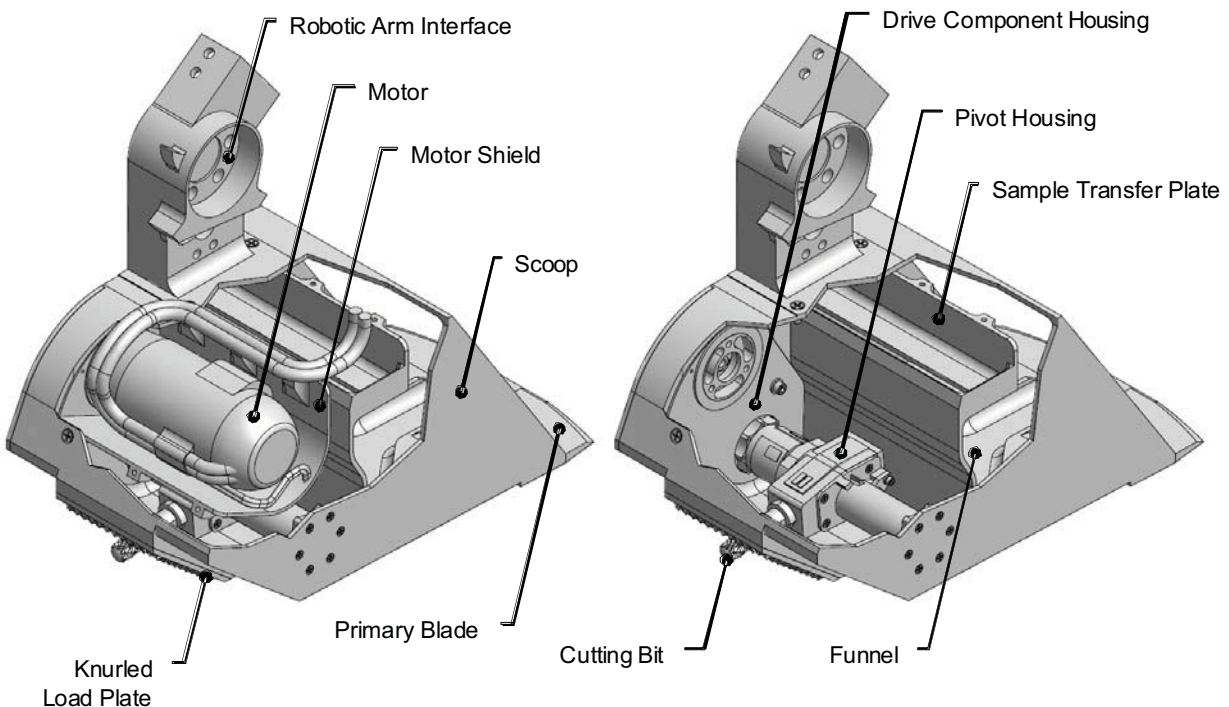


Figure 1. Cutaway of ISAD Showing Internal Components

The rear chamber of the ISAD contains a high-speed rasp cutting tool for penetrating the surface of hard icy soil, and acquiring the cuttings produced. Acquisition is accomplished by first preloading the ISAD scoop into the surface such that the spring-loaded cutting bit is forced into the scoop. A knurled contact plate grips into the icy soil preventing motion of the scoop and RA during rasp operations. The rasp cutting bit is then energized, resulting in rapid penetration of the surface, causing a plume of cuttings to ballistically enter the rear chamber of the scoop.

The tungsten carbide cutting bit is 6.35 mm in diameter and protrudes from the rear chamber through a 7.9-mm slot when the tool is in free space. The rasp cutting bit is mounted to a pivoting housing, which has a total stroke of 15°. Two hard stops prevent overtravel of this pivot housing. The “lower” hard stop limits the depth of penetration of the rasp cutting bit. The “upper” hard stop is positioned in order to allow the cutting bit to fully retract into the scoop. The pivot housing is spring loaded using a torsion spring. The torsion spring acts to force the cutting bit into the material, providing the necessary weight on bit of approximately 6 N for penetration of icy soil.

The rasp tool is driven by a brushed DC motor. The motor is powered by a current limited on-off circuit, which provides a maximum of 1.0 Amp, at 24.6 to 29.3 V. Accounting for frictional drag in the system, the actuator is able to produce 41 mNm of output torque at the rasp cutting bit and bit speeds of approximately 5300 RPM at room temperature. Torque is transferred from the motor shaft to the rasp cutting bit through a set of spur gears, and a pair of miter gears yielding an overall speed reduction of 1.25:1 from the motor to the bit. All gears are AGMA Q10, constructed of 15-5 PH stainless steel and age hardened to condition H1000. Figure 3 shows a cross section of a portion of the ISAD drivetrain. The cutting bit is supported on the upper end by a back to back angular duplex bearing pair while the lower end is supported by two shielded radial bearings. Another set of duplex angular bearings support the pivoting housing while three additional radial bearings support various drive train gears. All bearings are ABEC 7 and comprised of 440C stainless steel balls and races with phenolic retainers. All bearings and gears were grease plated with a solution containing 10 wt% Castrol Braycote[®] Micronic 600EF.

The device includes three resistive strip heaters that warm the mechanism to allowable operational temperatures. A 2.1-watt heater is attached to the motor, and two additional heaters, 2.7 watts and 1.6 watts are attached to the pivot housing. A temperature sensor on the motor provides ISAD temperature feedback. All components used to power the rasp cutting bit are thermally isolated from the main scoop body through the use of vespel as an insulating material. This minimizes heat transfer from the drivetrain components to the scoop sample transfer surfaces in an effort to reduce icy sample loss due to sublimation.

The cutting tool includes a set of features for producing vibration of the scoop surfaces. This vibration is essential for moving acquired sample from the rear chamber of the scoop to the front, and for improving the transfer efficiency from the front funnel to the instrument inlet ports. The vibration mechanism is only engaged when the rasp cutting bit is in its rest position against the “lower” hard stop. A cam feature attached to the rasp cutting bit engages a low-friction surface, which is grounded with respect to the scoop. As the rasp bit rotates at high speed, the cam feature causes the pivot housing to oscillate such that the spring loaded housing impacts the “lower” hard stop once per revolution, resulting in high frequency vibration.

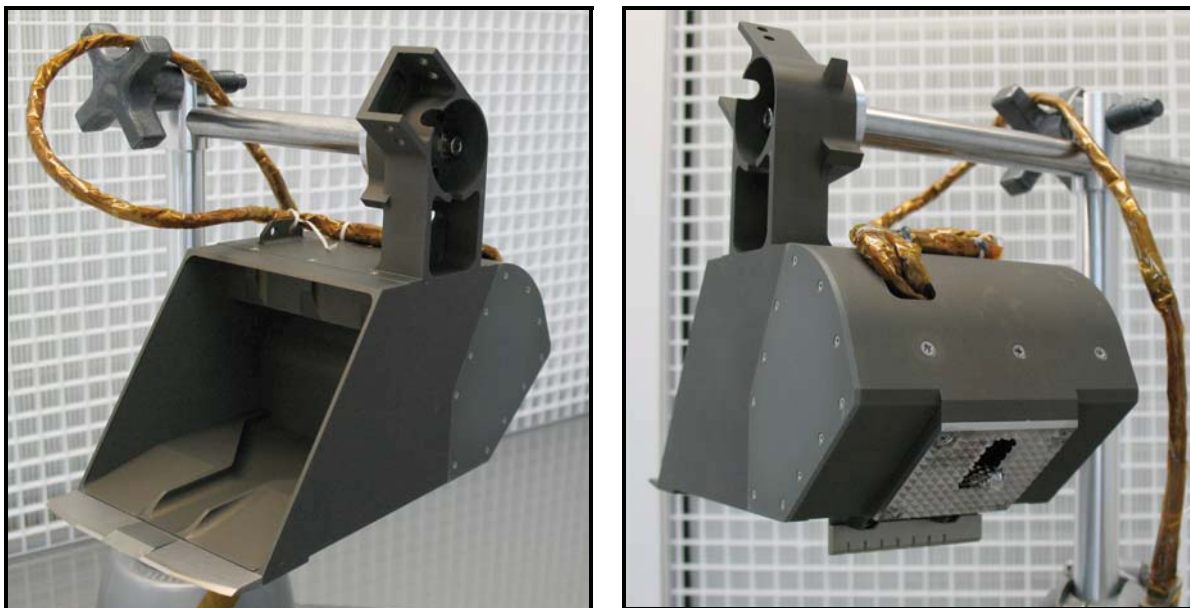


Figure 2. Icy Soil Acquisition Device Flight Unit on Assembly Fixture

The front and rear chambers of the scoop are separated by a sample transfer plate. During digging operations, this plate prevents the majority of scooped material from filling the rear chamber of the ISAD, which could result in jamming of the cutting tool. This plate also acts to move sample from the rear

chamber to the front chamber so that samples acquired using the rasp cutting tool can be dropped off to instruments in the same manner as bulk soil. The plate consists of a vertical and a horizontal shelf, with a slot in the horizontal shelf. This creates a labyrinth through which material can be transferred from rear to front by rotating the entire scoop about the Robotic Arm wrist axis. The sample transfer plate is made from 7075-T73 aluminum with a hard coat clear anodize for abrasion and wear resistance.

Once digging reveals hard icy soil, the secondary blade, located on the bottom of the scoop, may be used to prepare the surface for acquisition by the rasp tool, depending on the surface topography. This flat edged blade will scrape the icy soil to form a more uniform surface for placement of the ISAD. Once the surface has been prepared, the RA will place the ISAD such that the rasp tool is in contact with the target area. The RA will then preload the ISAD with a minimum preload of 40 N. The rasp cutting tool will then be energized for a period of approximately 30 to 60 seconds, resulting in acquisition of icy soil. The RA then relieves the preload on the ISAD and retracts it from the surface. Placement and acquisition can be repeated several times in different locations, depending on the amount of sample desired, and the spacecraft resources available. After all acquisition operations have been completed, the sample is transferred to the front of the scoop for imaging by the RAC, and drop-off to the analytical instruments. The transfer operation consists of a series of RA wrist motions to move the sample along a number of panels that divide the front and rear chambers of the scoop. During the transfer operation, the rasp cutting tool can be energized, inducing vibration to aid in the flow of particles.

Mechanism Design and Test Lessons Learned

High Speed Low Torque Seal Design

The Icy Soil Acquisition Device is a high speed, low torque sampling device. The Maxon REØ25 motor, coupled with a reduction ratio of 1.25 : 1, has a nominal output torque of 0.054 N·m (0.478 in·lb). In order to transfer the maximum possible amount of torque to the cutting bit, the frictional drag torque of the drivetrain needs to be minimized. Some sources of frictional drag in the mechanism's drivetrain include inefficiencies in spur and miter gear torque transfer, drag due to lubrication of bearings, and preloading of angular contact bearings. These effects can be minimized by tight tolerances and good assembly techniques, however the largest variability in a low torque mechanism's friction drag can come from the dust seal if not accounted for early in the design process.

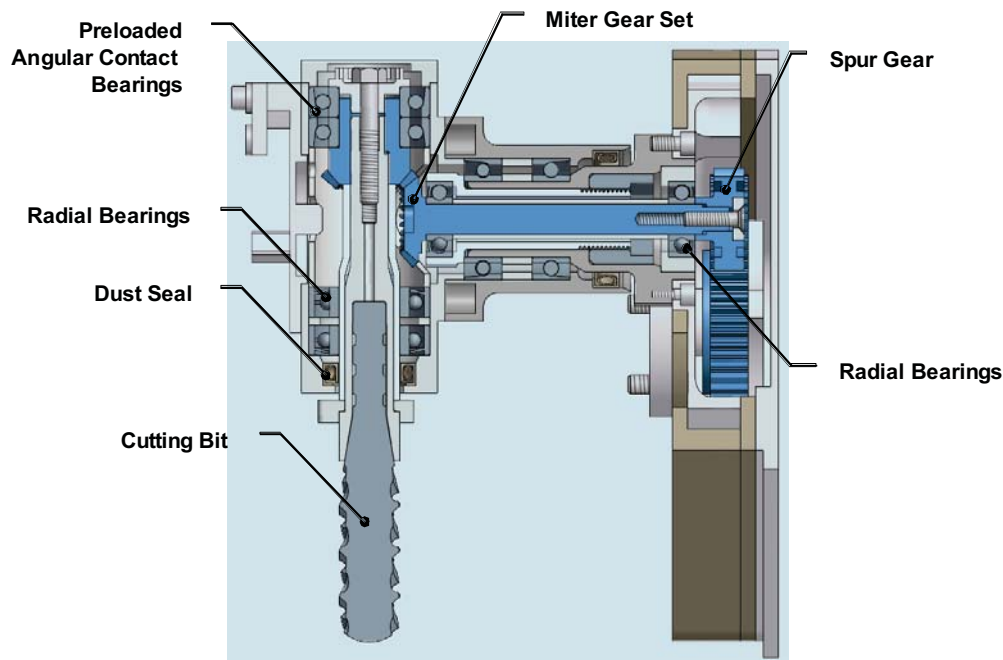


Figure 3. Drivetrain Cross Section Showing Dust Seal Location

As shown in Figure 3, the ISAD drivetrain utilizes a dust seal near the cutting bit to protect the critical internal components from dirt and dust migration. A custom canted coil spring energized seal was used for the dust seal, with Glass Filled Polytetrafluoroethylene Molybdenum Disulfide Reinforced (GFPM) polymer as the seal material, and 316 Stainless Steel as the backing and spring material. The shaft material on which the seal mates is 6Al-4V Titanium alloy.

When specifying a custom dust seal for a low torque application, it must be understood that manufacturers typically fabricate this type of seal to withstand high-pressure liquids and gases. As a result, spring energized seals are typically designed to be tight on the shaft, causing drag torques that can be a significant portion of the available torque when dealing with a mechanism such as the ISAD. With this effect in mind, the manufacturer was instructed to design the seal to a shaft diameter of 6.53 mm, when the actual shaft diameter was 6.34 mm. The difference was based on previous experience with high speed, low torque sealed mechanisms. When the seals were delivered, they were qualitatively determined to have an unacceptable amount of drag torque on the 6.34 mm Titanium shaft. This was expected, and material was removed from the shaft to reduce the frictional drag of the drivetrain. The required shaft diameter was determined by pressing the seal into the seal housing, and using hardened gage pins of varying size to find the optimal shaft size. By gently rotating the gage pin by hand, the technician could “feel” the difference in drag torque. This qualitative assessment of the drag torque resulted in the final diameter of the Titanium shaft being modified to 6.09 mm, a difference of 0.44 mm from what was originally specified to the manufacturer. This diameter produced the minimum amount of drag torque while maintaining a dust seal around the shaft. Subsequent testing performed on an identical seal revealed that the seal drag torque at room temperature on the 6.09-mm shaft was approximately 0.0035 N•m, while a 6.53-mm shaft would have produced a drag torque of about 0.018 N•m. After thermal dynamometer testing the Flight Model ISAD unit, the total drag torque of the mechanism was determined to be approximately 0.013 N•m at the low temperature operational extreme of -80 °C, and 0.007 N•m at room temperature (+20 °C). Had the manufacturer-recommended shaft diameter been used, the drivetrain drag torque would have increased by a factor of three at room temperature, leading to greatly reduced startup torque margin, and possible stalling of the mechanism at low temperatures.

When designing a custom spring seal for a high-speed low torque mechanism, it is difficult at best to determine the size of shaft, which will mate with a particular seal without having the seal in hand. Similarly, there is a large amount of risk associated with fixing the shaft diameter, and attempting to specify to the manufacturer the seal diameter to provide a dust seal while minimizing the amount of mechanism drag torque. The risk inherently lies with schedule and cost constraints, which were significant drivers in the development of the ISAD.

To minimize the impact on development schedule and project cost, the spring seal should be specified initially for a nominal shaft diameter. The shaft itself should be designed with the intention that material be removed once the spring seal, shaft and housing are in hand. This involves leaving enough material on the diameter of the shaft to allow for machining prior to final assembly of the mechanism. In this torque regime, it is critical that the shaft be matched to the actual seal press fit into the housing, as a slight variation in shaft diameter can make a substantial difference in the drag torque.

An additional observation related to the seal was noticeable change in frictional drag after exposing the mechanism to the high end of the required temperature range during thermal vacuum contamination control bakeout. While GFPM is rated for temperatures safely exceeding the +110 °C maximum that the ISAD was subjected to during thermal cycling, a noticeable difference in drag torque was observed after soaking for 8 hours at this temperature. Specifically, an additional 0.004 N•m of torque (approximately 10% of actuator output capability) was measured indirectly by considering the additional motor current to drive the mechanism under “no-load” conditions with the vibration feature disengaged. This observation was consistent for both the engineering and flight units. Initially it was not clear that this additional frictional drag was due to the GFPM seal. Since the change in drag did not warrant disassembly of the mechanism for inspection of this component, the seal could not be completely confirmed to be the root cause. However, all other possible scenarios were deemed highly unlikely. The seal hypothesis was supported by the fact that the drag slowly decreased to normal levels after several minutes of operation. Assuming the seal was the source of the additional drag, the reason for its change in behavior could be: (1) a slight tightening of the GFPM seal on the shaft due to pressure applied by the canted spring; (2) a change in the frictional properties of the GFPM-on-titanium material combination due to out gassing of

volatiles or (3) a combination of both effects. For mechanisms that are sensitive to slight increases in drag torque, it is recommended that mechanism designers experiment with these spring energized seals at the expected environmental conditions prior to finalization of the design.

Cam Actuated Vibration Mechanism Design

The ISAD includes a unique method of producing the vibration necessary for moving particles across sample transfer plates within the scoop. To the best of the authors' knowledge, this cam vibration mechanism is unlike any other flight-qualified device, and the design contains several important features that contribute to its successful operation. This type of mechanism can be utilized on future planetary sampling systems where vibration is required to aid the flow of particles.

The cam vibration mechanism utilizes a spring preloaded pivoting assembly to produce an impact force on the base of the ISAD scoop. Figure 4 shows the "Pivot Housing" in its rest state, with the mechanism un-powered. In this state, the "Cutting Bit" is in the fully extended position, and the pivot housing is fixed against the "Lower Hardstop". As the cutting bit rotates, the "Cam" gradually engages the "Bumper", raising the pivot housing off of the lower hardstop, against the direction of torsion spring preload. As the cam and cutting bit rotate further, a change in the cam geometry causes the cam to suddenly disengage from the bumper. This releases the preloaded pivot housing, allowing it to impact against the lower hardstop. This impact is directly coupled with the rotation speed of the cutting bit, and results in an approximately 90 Hz frequency. Both the cam and the bumper are individual components that can be changed out without affecting the design of surrounding hardware. This minimizes schedule risk, as cam and bumper design can proceed without delaying fabrication of mating hardware.

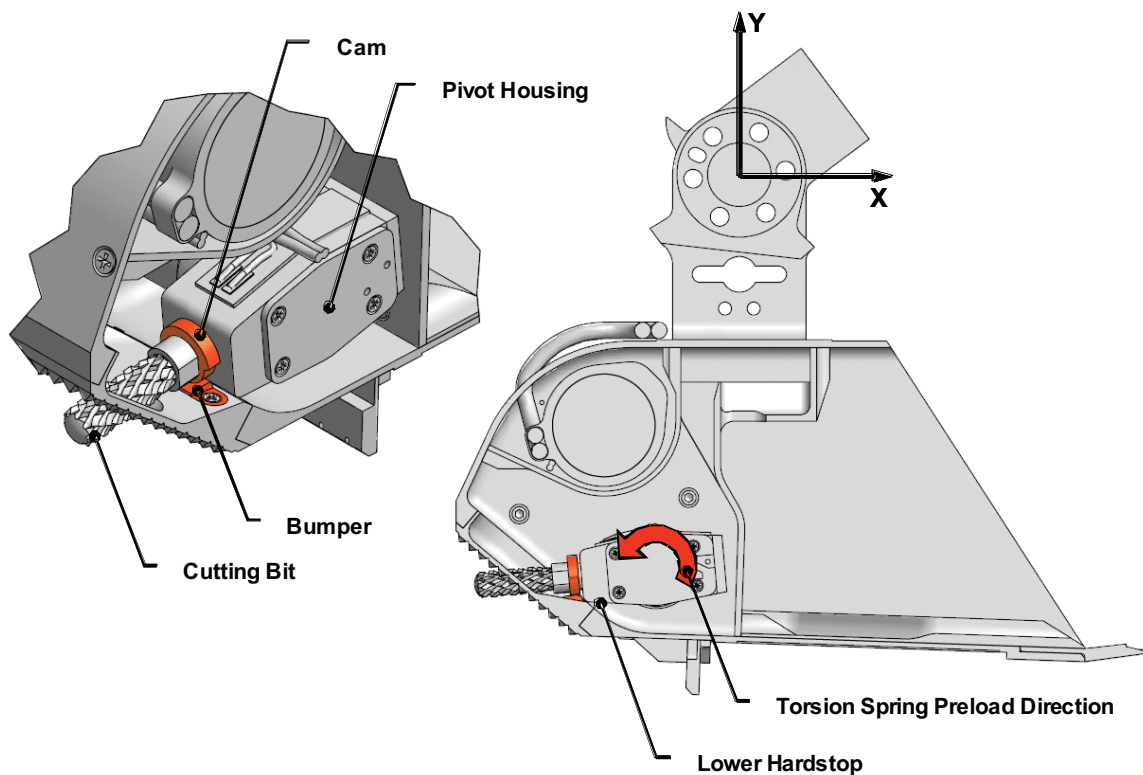


Figure 4. Cam Vibration Mechanism Section View

The primary challenge of a cam-actuated vibration mechanism is designing the interface between the cam and the bumper to function throughout the expected lifetime of the device. Gradual wear of the cam and bumper will ultimately degrade the ability to produce vibration. Material choices, cam and bumper geometry and surface treatments all contribute to the functionality of the mechanism as it nears the end of its required operational life. The cam vibration mechanism on the ISAD was required to function for a total

number of output revolutions of 383,000. Due to the unique nature of the device, a demonstration of two times life was required to prove flight worthiness.

The geometry of the cam was an important consideration in the design. Figure 5 shows the wear of an early prototype cam made from 17-4 PH Stainless Steel age hardened to condition H900 with no surface treatment. This cam interfaced with a bumper made from 50% cold worked Nitronic 60. These parts were designed for simplicity of fabrication in a short amount of time, and minimal consideration was given to the cam geometry. The wear shown in the images occurred after one hour of operation at 5300 RPM (approximately 318,000 output revolutions). These tests were performed in a vacuum chamber at Mars ambient conditions on a test fixture with similar geometry and rotational speed as the flight ISAD design. The vibration produced at the end of the test was insufficient to fluidize even dry particles. These images show the importance of geometry and material selection to the overall success of a cam-actuated vibration mechanism. The combination of 17-4 PH and Nitronic 60 is typically used to minimize galling and wear in sliding friction applications. In this application, the high speed and abrupt impact quickly deteriorated both materials.

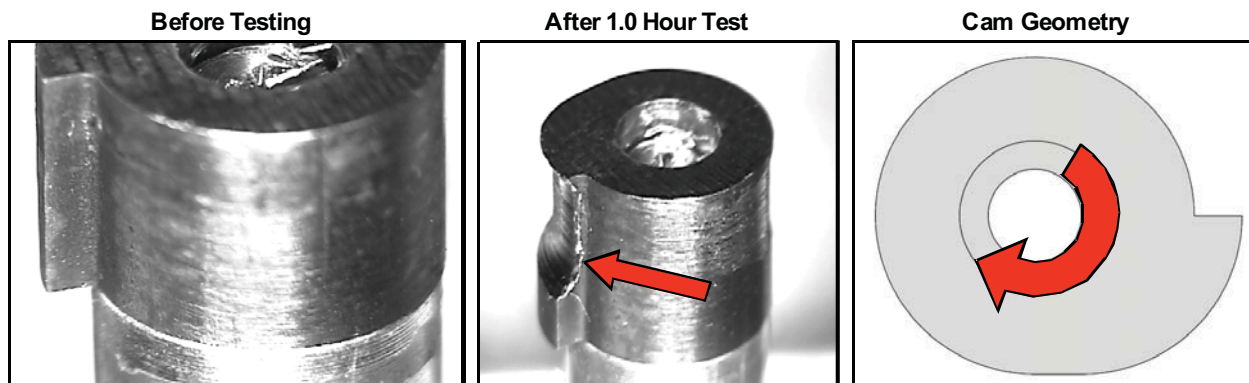


Figure 5. 17-4 PH Prototype Cam Wear and Geometry

As shown in Figure 5, the geometry of the prototype cam was not optimized to deliver a smooth transition between the minor diameter of the cam and the major diameter. The transition was abrupt, and occurred in the final quarter rotation of the cam. The flight cam design utilizes a cycloidal cam profile to gradually transition from the minor diameter to the major diameter through three quarters of a rotation. Cycloidal cam geometry is used in cam design where a sinusoidal acceleration profile is desired to minimize reaction loads. Equation 1 shows the desired cam acceleration profile. The displacement profile can be determined through integration and application of boundary conditions. The formula for the radius of the cycloidal cam profile is shown by Equation 2.

$$a = C \sin 2\pi \left(\frac{\theta}{T} \right) \quad \text{Equation 1}$$

$$r = \left[r_{ROOT} + \left(\frac{h\theta}{T} \right) \right] - \left[\left(\frac{h}{2\pi} \right) \sin \left(\frac{2\pi\theta}{T} \right) \right] \quad \text{Equation 2}$$

r = Cam radius , r_{ROOT} = Minor radius of cam, h = Distance between major and minor radius of cam
 T = Period of cam

Age-hardened Vascomax C-300 Stainless Steel was chosen as the material for both the cam and the bumper due to its superior strength and hardness (52 Rockwell "C"). In addition, a low-friction electroless nickel coating from General Magnaplate (Magnaplate HMF) was used as a surface treatment on both the cam and bumper to reduce frictional effects, and improve surface hardness at the contact interface.

Figure 6 shows post-test images of a cam of identical geometry, material and surface treatment as the flight unit cam vibration mechanism. This cam, along with a flight-like bumper was tested in a Mars ambient environment to approximately 780,000 revolutions, two times the required life of the mechanism. The test was performed in several segments on a prototype ISAD with similar sample transfer plates and geometry as the flight ISAD. After each segment, a known mass of dry sample was placed in the rear chamber. Using the cam vibration mechanism, the material was transferred to the front of the scoop, where the mass was again measured. After a demonstration of two times the required life, the efficiency of sample transfer using the cam vibration mechanism did not show any signs of degradation, remaining at 90% or greater. As shown in Figure 6, there was minimal wear to the surface treatment at the end of the test, preserving the cycloidal geometry and the ability to produce vibration. The bumper showed similar minimal signs of wear. During the lifetime test, a witness plate was used to capture the material worn away by both cam and bumper. Comparing the measured mass of the worn material to the total calculated mass of the “ramp” portion of the cam, less than 10% of the ramp was worn away. This combination of material and geometry produced a cam vibration mechanism, which will continue to generate vibration well past the required operational life.

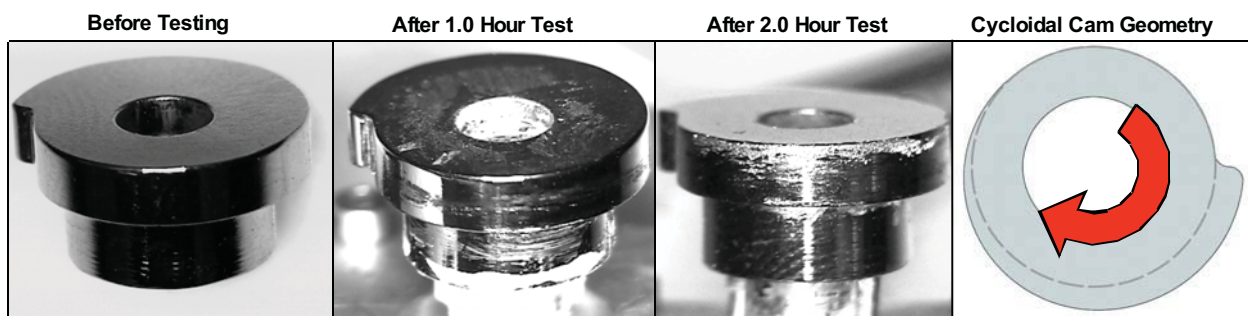


Figure 6. Cycloidal Cam Geometry

Small Form Factor Braze Joint for High Load Capacity

The cutting bit of the ISAD is a modified commercially available tungsten carbide rasp bit typically used in ceramic tile applications. A consumer rasp bit was selected due to budget and schedule risks associated with designing and testing custom cutting bits. A variety of bits were tested early in the design process, and a selection was made which provided the best sample production performance in dry analog material. For assembly purposes, a decision was made to vacuum furnace braze the cutting bit to a stainless steel shank to allow the use of threaded fasteners as a connection mechanism.

The ISAD cutting bit protrudes from the rear of the scoop when in the rest position. This results in exposure of the bit to potentially high loads during trench digging operations, and icy surface scraping operations with the secondary blade. As shown in Figure 4, during digging or scraping operations, the ISAD is translated in the “X” direction. To reduce the risk of damaging the bit and drivetrain during these sequences, the Pivot Housing is designed to retract automatically into the scoop if inadvertent loads are applied to the bit while digging or scraping. During these operations, loading of the ISAD is not limited to the X-Y plane. The Robotic Arm can impose lateral loads in the ISAD “Z” direction of up to 50 N. There is no retraction mechanism for the cutting bit to absorb loading in this direction, and although the lateral loads are small compared to those sustained by the structure in the X-Y plane, they are large enough to risk damaging the brazed connection of the cutting bit.

The ISAD cutting bit is only 6.35 mm (0.250 in) in diameter, due to limitations in the amount of torque available, and the desire to run at high speeds to increase sample acquisition productivity. This limited the selection of braze joint form factors to those that could be fabricated with the amount of material available on the cutting bit shaft. Due to the high speed nature of the design, minimizing shaft runout was desirable to reduce imbalance of the mechanism. The exposure to high lateral loads, and the brittle nature of tungsten carbide added further complexity to the design. A number of distinct features were incorporated into the braze joint design to minimize stresses in the connection while maintaining shaft runout between the cutting bit and stainless steel shank. These features can be applied to brazed connections for similar high speed, small form factor applications.

Figure 7 illustrates a prototype braze joint which was fabricated and load tested. Due to packaging constraints, it was necessary to reduce the diameter of the carbide bit to fit into the stainless steel shank. Three grooves in the bit provide for mounting of gold-nickel alloy wire to act as filler metal for the braze joint, but also decrease the overall strength of the tungsten carbide bit. The dimensions of these preform grooves is dependent on the amount of filler metal required to coat the surface of the braze joint. A loose radial clearance in this region between the bit shaft and the shank allows for braze filler metal to flow. The joint also includes an alignment feature near the base of the cutting bit teeth which controls shaft runout, but does not allow a sufficient gap for braze filler metal to reinforce the connection. Figure 8 shows the completed braze joint after having performed load testing. The joint was sectioned in order to view the internal braze penetration. Cracks at each of the three preform grooves are evident in the figure. Whether load testing, or the act of sectioning the joint was the cause for these cracks is unknown, however it is clear that the aspect ratio of depth to height of the preform grooves resulted in a high stress concentration at the base of these features, and failure of the brittle tungsten carbide shaft.

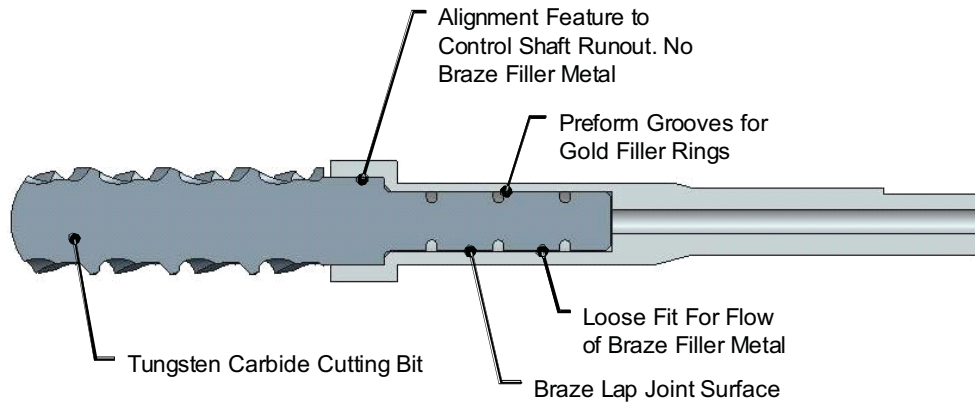


Figure 7. Prototype Cutting Bit Braze Joint Design

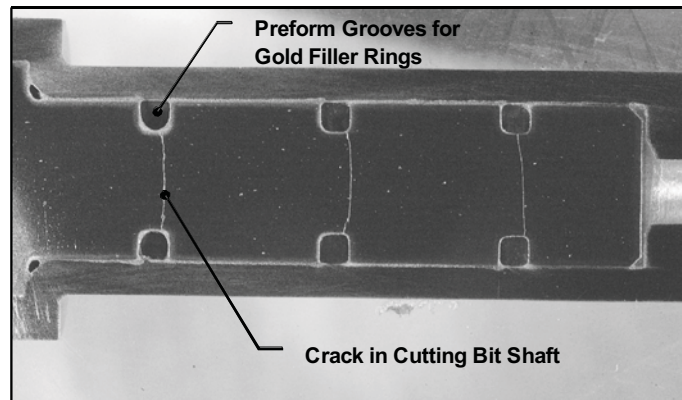


Figure 8. Prototype Cutting Bit Braze Joint Section Showing Cracks in Bit

The braze joint implemented on the flight ISAD unit utilizes the same cutting bit as the prototype design, but includes a number of improved geometric features for decreasing stress and controlling shaft runout. Figure 9 shows the final design of the braze joint. The material selected for the bit shank was 15-5 PH Stainless Steel. The material selected for the braze alloy was 82% gold and 18% nickel. Following the completion of the braze operation, the entire assembly was precipitation hardened to Condition H1000 to harden and strengthen the shank.

Compared to the prototype design, the aspect ratio of the preform grooves was changed to minimize stress concentrations at the base of the groove. Gold bands were used rather than gold rings, resulting in

shallower and wider grooves while maintaining the necessary volume of filler metal. This significantly reduces the stress concentration at the grooves. This design also incorporates a tapered transition between the outer diameter of the bit and the reduced diameter at the braze joint. This provides for ease of assembly while minimizing the stress concentration due to the change in geometry. To further strengthen the joint, a shallow recess in the tapered region allows braze filler metal to flow into the tapered region. To control runout of the bit, a tightly tolerated region at the base of the cutting bit allows the bit to maintain concentricity with the stainless steel shank during assembly and throughout the braze cycle.

These minor changes in geometry help to increase the load capacity of the brazed joint. The brazed joint survived a lateral load of 50 N applied at the tip of the cutting bit, with a proof load factor of 1.2. High-resolution X-Ray images of the joint confirmed that no cracks formed as a result of load testing, and that braze filler material penetrated all lap joint connections, including the tapered region. It should be noted that during the brazing process, the cutting bit was facing up with respect to gravity, demonstrating that capillary action alone allowed braze filler metal to flow into the tapered recess area, further strengthening the joint. Running the bit at its peak speed of approximately 5300 RPM and visually observing the runout confirmed that concentricity between the cutting bit and the shank had been maintained. Figure 10 shows the brazed assembly.

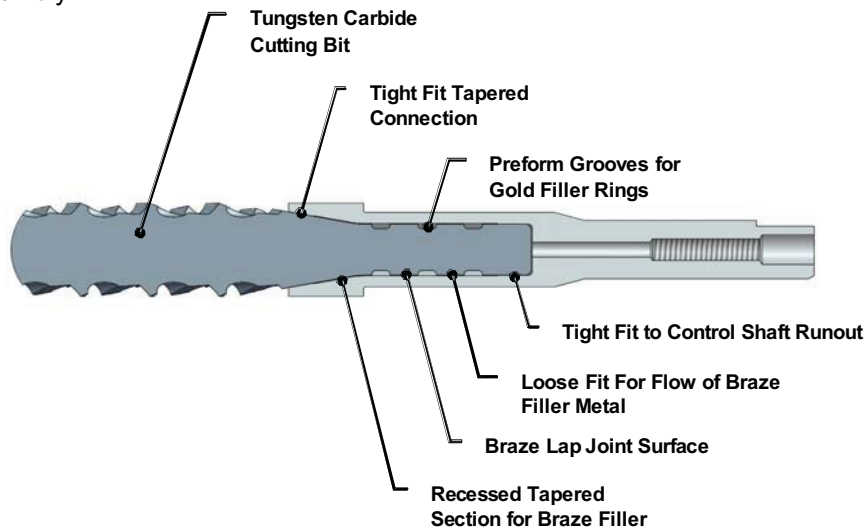


Figure 9. Flight ISAD Cutting Bit Design

When designing small form factor braze joints exposed to high load conditions and consisting of one or more brittle materials, it is important to minimize stress concentrations around geometry transitions, and to reinforce these transition areas with braze metal whenever possible. This braze joint is optimized for the geometry and material constraints imposed by the ISAD design. Had these factors, in addition to budget and schedule limitations not been present, the design may have taken a less involved approach, possibly utilizing a solid tungsten carbide shaft rather than a braze connection, or a less brittle material for the cutting bit.



Figure 10. Flight ISAD Braze Joint

Torsion Spring Design

During a sample acquisition operation the load plate on the ISAD is preloaded against the target by the RA, and the rasp bit retracts into the scoop body, applying a preload (or “weight-on-bit”) to the soil. This weight-on-bit is produced by a torsion spring. In its free state the rasp cutting bit protrudes from the back of the ISAD scoop and is preloaded by the spring against an internal hard stop that provides 5.0 N of weight-on-bit at the bit tip. When loaded against a soil target the bit pivots into the back of the ISAD to a maximum deflection of 15° and applies 6.6 N of weight-on-bit at the bit tip. This weight-on-bit range was selected based on the ability of the bit to penetrate into frozen Mars soil analog targets to the full depth of the tool and to meet the actuator startup torque margin requirement. Generally, increasing the weight-on-bit of the rasp decreases torque margin but increases the ability to penetrate hard icy soils, so a compromise between the two was required.

The spring is made from 1.5-mm (0.059-in) diameter 17-7 PH stainless steel wire that has been age hardened, shot peened and passivated. The spring has 12 coils with an 11.1-mm (0.438-in) coil outer diameter. One leg of the spring is formed tangential to the coil and the other axially aligned with the coil. Since the spring assembly is directly in line with the soil particle transfer path, both the coil diameter and leg geometries were constrained in volume and shape so as to allow unhindered particle flow underneath the assembly. To reduce the potential for jamming by foreign debris, the spring coils were covered by a protective housing that was integral with the spring mount. The spring coil inner diameter is constrained by an aluminum arbor with a General Magnaplate TUFAM wear resistant surface treatment.

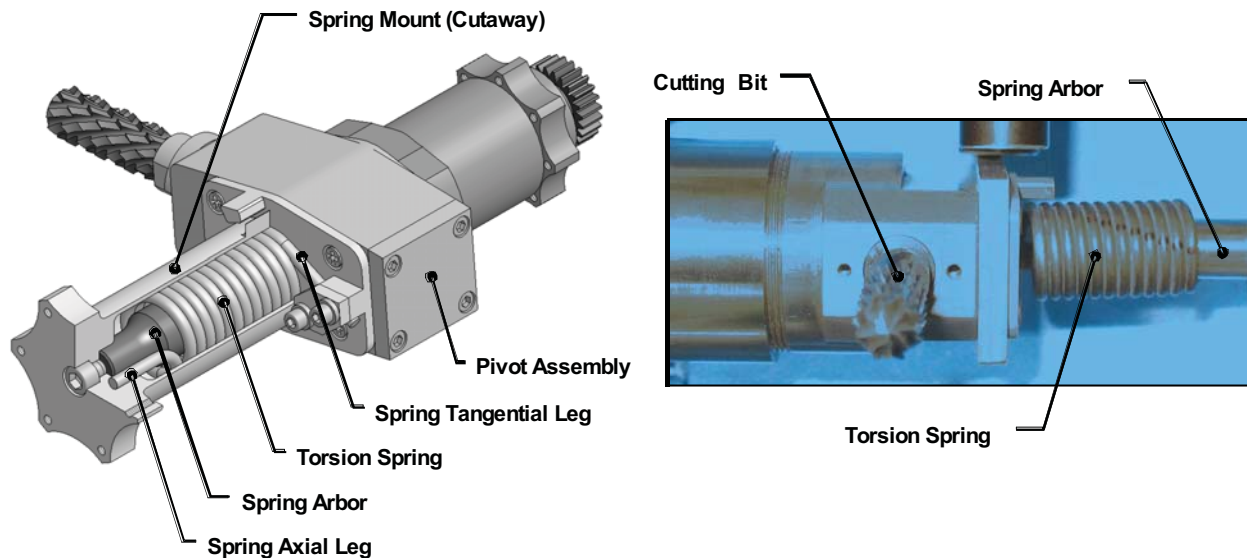


Figure 11. (Left) ISAD Pivot and Spring Assemblies; (Right) ISAD Spring Test Fixture

The spring was designed to produce a change in weight-on-bit over the 15° bit pivot stroke of 0.7 N. Such a narrow range of weight on bit was desired to maintain sample acquisition performance over the entire stroke of the cutting bit. The ISAD flight unit spring produces a change in weight-on-bit of 1.6 N over the 15° stroke, a difference of 0.9 N between the theoretical and actual values. This difference is a combined result of the spring manufacturing and integration processes. The spring rates of the springs provided by the manufacturer were slightly higher than that called out in the manufacture drawing (0.023 in-lb/° actual compared to 0.019 in-lb/° theoretical), which yields an increase of approximately 0.3 N over the stroke of the bit. The remaining 0.6-N difference between the actual and theoretical weight-on-bit values is attributed to friction in the spring assembly and the accuracy of the test method. Some of the springs also had non-linear torque versus deflection curves and there was some variability in both the slope and offset of this curve. In addition to spring rate differences, there were small variations in the axial leg geometries of the springs, such as leg straightness, the angle at which the leg protrudes from the coil, and the radius of the axial leg bend. The leg straightness and bend radius had an effect on the fit of the spring into the outer housing and the geometry of the assembled spring when wound up. As seen in Figure 11, when

wound up the coil tends to pivot about the axial leg anchor point and move out of alignment with the arbor. This misalignment can cause the spring to contact the arbor, housing or both, which increases friction in the assembly, resulting in a higher spring rate.

It was anticipated that there would be variability among the as-received springs. Therefore, five times as many springs were fabricated than were required in the delivered ISAD units. This provided the ability to choose the best springs out of the lot to be integrated into the ISAD units. The springs integrated into the ISAD units were selected based on having a minimal and constant spring rate and acceptable axial leg geometries. Since there is significant variability from spring to spring, each spring had to be “tuned” appropriately for each ISAD unit. To achieve a desired range in weight-on-bit from a particular spring, the mounting hole location in the spring mount for the spring’s axial leg was determined following testing of that spring in a custom test fixture. As stated, the ISAD flight unit weight-on-bit range is 5.0 N to 6.6 N, which was measured at room temperature. Tests conducted with the mechanism soaked at -80°C yielded weight-on-bit values of 5.5 N to 8.2 N over the 15° stroke of the bit, an increase of 1.1 N over that measured at room temperature. This increase is attributed to added friction in the spring assembly at cold temperatures as well as a potential increase in the spring stiffness.

When considering a custom torsion spring to provide a narrow range of output torques at specific deflection angles, there are many sources of error between the theoretical design and the actual performance. If a torsion spring is required to operate within a precise performance range it is important that sufficient margin be accounted for in the design so that deviations in spring performance due to the manufacturing process, mounting method and assembly process do not adversely affect mechanism performance. For future mechanisms, it is recommended that the use of an axially aligned torsion spring leg be avoided when variability in performance is undesirable. An axially mounted leg is sensitive to both the spring mounting scheme and the assembly procedure. In the case of the ISAD, spring preload directly affected the actuator torque margin and bit productivity. A specific range was desired, but the spring was successfully implemented in the design by fabricating a relatively large batch of springs that could be selected from to find the best match for each unit and by waiting until the spring was selected before locating mounting holes for the axial leg.

Conclusion

The ISAD is a first of its kind device to be qualified for space flight. Many aspects of the design are unique, but can be applied to future spacecraft mechanisms. The highly constrained requirements space resulted in the use of a number of unconventional design features and methods, while schedule and budget restrictions played a large factor in many design decisions.

Designing a low torque mechanism while preventing debris migration from damaging sensitive drive components requires knowledge of the effects of the dust seal on the overall frictional drag of the mechanism. Depending on available torque margin, shafts that interface with dust seals may require modification to minimize seal drag. Seal behavior across the environmental range should also be characterized before design finalization.

A cam-actuated vibration mechanism is an effective means of inducing vibration to help fluidize both dry and ice-bearing soils and powders. The limitation on the overall life of the mechanism is the interaction between the cam and the bumper. Proper material, surface treatment and geometry selection is critical to extending the lifetime of the device.

Designing a small form factor braze joint for brittle material to sustain high load conditions involves careful consideration of the connection geometry. Materials such as tungsten carbide require gradual changes in geometry, and reinforcement with braze filler material to sustain high loads. Abrupt geometry transitions can result in failure of the joint when load is applied.

Use of torsion springs in a mechanism where a narrow range of output torque is required should be avoided. If space or packaging constraints dictate the use of a torsion spring, the spring should be designed using legs that exit the spring tangentially, rather than aligned with the spring axis. An axially aligned leg imposes a high degree of unpredictability on the output torque due to frictional effects

between the spring, the housing and the shaft. Significant torque margin should be applied to the spring design to account for these effects.

Acknowledgments

The authors would like to thank all of the ISAD program technicians, machinists, designers, engineers and managers at Honeybee Robotics and JPL for their commitment to developing this device. Specifically, the authors would like to thank Mark Balzer, Don Lewis, Don Noon and Greg Peters all of JPL for their time and technical insights.

This work was performed under a contract with Jet Propulsion Laboratory, California Institute of Technology, for the National Aeronautics and Space Administration. References herein to any specific commercial product, process or service by trade name, trademark, manufacturer, or otherwise does not constitute or imply its endorsement by the United States Government or the Jet Propulsion Laboratory.